

AD-A049 437

COLD REGIONS RESEARCH AND ENGINEERING LAB HANOVER N H
HEAT TRANSFER OVER A VERTICAL MELTING PLATE, (U)

F/G 13/1

DEC 77 Y YEN, M M HART

UNCLASSIFIED

CRREL-77-32

NL

1 OF 1
AD
A049437



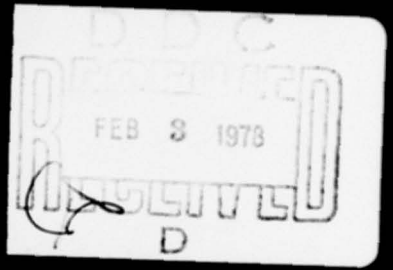
END
DATE
FILMED
3 - 78
DOC

AD A049437
CRREL
REPORT 77-32



Heat transfer over a vertical melting plate

AD A049437



$$Nu = A (Re_L)^m (Pr)^n$$

DISTRIBUTION STATEMENT A

Approved for public release;
Distribution Unlimited



*For conversion of SI metric units to U.S./British
customary units of measurement consult ASTM
Standard E380, Metric Practice Guide, published
by the American Society for Testing and Materials,
1916 Race St., Philadelphia, Pa. 19103.*

CRREL Report 77-32

Heat transfer over a vertical melting plate

Yin-Chao Yen and Mark M. Hart

December 1977

ACCESSION FOR	
REF	White Sarcas
DDC	Soft Sarcas
ORIGINATED	
JUSTIFICATION	
BY	
DISTRIBUTION/AVAILABILITY CODES	
DIST.	AVAIL. AND/OR SPECIAL
A	
A	
A	

D D C
DRAFTED FEB 3 1978
RECORDED

CORPS OF ENGINEERS, U.S. ARMY
COLD REGIONS RESEARCH AND ENGINEERING LABORATORY
HANOVER, NEW HAMPSHIRE

Approved for public release; distribution unlimited.

Unclassified

SECURITY CLASSIFICATION OF THIS PAGE (When Data Entered)

REPORT DOCUMENTATION PAGE		READ INSTRUCTIONS BEFORE COMPLETING FORM
1. REPORT NUMBER 14 CRREL Report-77-32	2. GOVT ACCESSION NO.	3. RECIPIENT'S CATALOG NUMBER
4. TITLE (and subtitle) 6 HEAT TRANSFER OVER A VERTICAL MELTING PLATE	5. TYPE OF REPORT & PERIOD COVERED	
7. AUTHOR(s) 10 Yin-Chao Yen and Mark M. Hart	6. PERFORMING ORG. REPORT NUMBER	
9. PERFORMING ORGANIZATION NAME AND ADDRESS U.S. Army Cold Regions Research and Engineering Laboratory Hanover, New Hampshire 03755	10. PROGRAM ELEMENT, PROJECT, TASK AREA & WORK UNIT NUMBERS 16 DA-Project 4A161191A91D	
11. CONTROLLING OFFICE NAME AND ADDRESS U.S. Army Cold Regions Research and Engineering Laboratory Hanover, New Hampshire 03755	12. REPORT DATE 11 December 1977	13. NUMBER OF PAGES 18
14. MONITORING AGENCY NAME & ADDRESS (if different from Controlling Office) 12 DOD	15. SECURITY CLASS. (of this report) Unclassified	
16. DISTRIBUTION STATEMENT (of this Report) Approved for public release; distribution unlimited.		
17. DISTRIBUTION STATEMENT (of the abstract entered in Block 20, if different from Report)		
18. SUPPLEMENTARY NOTES		
19. KEY WORDS (Continue on reverse side if necessary and identify by block number) Heat sinks Heat transfer Ice Melting		
20. ABSTRACT (Continue on reverse side if necessary and identify by block number) An experimental study of forced convective heat transfer over a vertical melting plate has been conducted. This study covers water velocities ranging from 1.7 to 9.8 mm/s and bulk water temperatures from 1.11 to 7.50°C. The experimental results are correlated in terms of Nusselt, Prandtl and Reynolds numbers with a moderate correlation coefficient of 0.843. The results are expected to be useful in predicting the heat transfer characteristics of a much larger prototype ice-water heat sink.		

PREFACE

This report was prepared by Dr. Yin-Chao Yen, Chief, Physical Sciences Branch, Research Division, U.S. Army Cold Regions Research and Engineering Laboratory, and by Mark M. Hart, formerly an engineering assistant at CRREL. The work was sponsored by DA Project 4A161101A91D, *In-House Laboratory Independent Research*.

William Quinn and Dr. Yoshisuke Nakano technically reviewed the manuscript of this report.

CONTENTS

	Page
Abstract	i
Preface	ii
Nomenclature	iv
Summary	v
Introduction	1
Problem	1
General review of the subject	1
Experimental apparatus	2
General considerations	2
Water reservoir	2
Test chamber assembly	2
Pumping system	4
Electrical control system	5
Experimental procedure	5
Experimental results	6
Discussion and comparison of results	9
Conclusions	12
Literature cited	12

ILLUSTRATIONS

Figure

1. Schematic of the experimental setup	3
2. Schematic of the ice frame	4
3. Melting rate as a function of bulk water temperature	6
4. Relation between Nu_L/Pr and Re_L	8
5. Comparison of present data with computed values from horizontal plate	10
6. Comparison of present data with those from free convection studies	11

TABLE

Table

1. Experimental parameters and computed results	7
---	---

NOMENCLATURE

<i>A</i>	area of melting surface
<i>a_n</i>	defined by eq 4
<i>a₀</i>	defined by eq 6
<i>B</i>	a constant
<i>c</i>	specific heat of water
<i>g</i>	gravitational acceleration
<i>Gr</i>	Grashof number, $[gL^3 \beta_{\infty}(T_p - T_{\infty})] \nu^2$
<i>h</i>	average heat transfer coefficient
<i>k</i>	thermal conductivity of water
<i>L_f</i>	height of the ice sample
<i>L</i>	latent heat of fusion of ice
<i>M</i>	melting rate
<i>Nu_L</i>	Nusselt number (<i>hL</i>)/ <i>k</i> with melting
<i>Nu₀</i>	Nusselt number without melting
<i>Pr</i>	Prandtl number as <i>cμ/k</i>
<i>q_f</i>	heat used for melting
<i>q_s</i>	sensible heat
<i>R</i>	radius
<i>Re_L</i>	Reynolds number, $(\nuρL)/μ$
<i>T_i</i>	initial ice temperature
<i>T_∞</i>	bulk water temperature
<i>T_m</i>	melting temperature
<i>T_p</i>	plate temperature
ΔT	temperature difference (<i>T_∞-T_m</i>)
<i>v</i>	water velocity
<i>v_x</i>	velocity along the plate
<i>W</i>	amount of ice melted
<i>x</i>	coordinate along the plate
<i>y</i>	coordinate perpendicular to the plate
<i>α</i>	thermal diffusivity of water
<i>β</i>	defined as <i>c(T_∞-T_m)/L_f</i>
<i>β_∞</i>	defined by eq 15
<i>θ</i>	time
<i>μ</i>	viscosity of water
<i>ν</i>	kinematic viscosity
<i>ρ</i>	density of water
<i>ρ_i</i>	density of ice
<i>τ₀</i>	shear stress at the interface without melting
<i>τ_w</i>	shear stress at the interface with melting
<i>λ</i>	a dummy variable

SUMMARY

An experimental device was developed to simulate the heat transfer behavior of a rather large prototype ice-water heat sink. Since both the laboratory setup and the prototype heat sink used the same fluid medium (i.e. ice-water), it would have been nearly impossible to provide the dynamic similarity needed to ensure that the laboratory work would reproduce heat transfer characteristics of the prototype. This difficulty was circumvented by installing belts on two opposite sides of the square test column. The belts were designed and adjusted to move at the same direction and velocity as the water flowing through the test chamber. In doing this, the laboratory setup could be considered as a segmental ring cut from the proposed prototype.

The experiments covered bulk water temperatures ranging from 1.11° to 7.50°C and water velocities from 1.7 to 9.8 mm/s. The experimental results can be expressed in terms of Nusselt, Prandtl and Reynolds numbers as $Nu_L/\text{Pr} = 3.275(\text{Re}_L)^{0.270}$ with a moderate correlation coefficient of 0.843. The results were also compared with those computed from the case of laminar heat transfer over a horizontal melting plate. It was found that the results were four to five times higher than those for the horizontal plate.

From this study it was also concluded that, for the case of forced convective melting heat transfer, the effect of buoyancy force created by maximum density at 4°C on heat transfer appeared insignificant even at the lowest velocity (i.e. 1.7 mm/s) conducted in this investigation. The heat transfer was drastically reduced in the vicinity of about 5.6°C in the case of free convective melting heat transfer for a wide variety of melting geometries.

HEAT TRANSFER OVER A VERTICAL MELTING PLATE

Yin-Chao Yen and Mark M. Hart

INTRODUCTION

Problem

Ice has been considered as a heat dissipating medium for enclosed generating systems, and considerable interest has been devoted to investigating the feasibility of using ice in heat sinks for underground hardened military installations. These sinks would be used in an emergency situation to absorb the waste heat created by an underground power generating station and its associated support facilities. During most of a power plant's operation, heat rejection is accomplished at the ground surface with typical cooling towers and water reservoirs, but a system that is capable of absorbing all the waste heat for a short period of time must be available at a moment's notice. A typical installation would consist of a nuclear steam turbine generator, a steam condenser and three ice-water heat sinks. One concept in particular uses cylindrical ice columns of 33.5 m height and 19.8 m diameter, with a circulating coolant rate of 9.08×10^5 kg/h and a minimum anticipated heat rejection rate of 6.73×10^6 kcal/h (see reference 2).

Brown and Quinn² studied such a heat sink by geometrically scaling their experimental setup to the actual 33.5-x 19.8-m prototype with a cylindrical block of ice 1.83 m in height and 1.22 m in diameter. Since the same fluid (ice-water) was used for both the model and the prototype sink, it was impossible to devise a model with total similarity to the prototype. They developed a scale model taking into consideration temperature, heat transfer and time factors, in addition to geometrical and performance characteristics, as a basis of analysis for the prototype. The results of the experimental model studies were compared with those predicted from numerical computation of the system. Favorable comparison was obtained, providing confidence in using model study results to calculate the prototype performance. Stubstad and Quinn³

investigated this problem further by conducting a larger scale experiment using an ice cylinder 3.0 m in height and 1.83 m in diameter. Both studies have provided a quantitative description of the melting pattern as a function of operating time.

In a more recent study, Grande⁴ presented an analysis and development of the conceptual design of an ice-water heat sink system to accommodate the closed cycle operation of a 1500-kW nuclear power plant in a hardened underground installation. This study provided a critical review of previous work on ice-water heat sinks. It also extended the analytical description of the sink's thermal performance and assessed the available options for varying the flow path of coolant water within the sink. Computer programs were developed for predicting the time histories of heat sinks in conjunction with power plants, and a practical sink design was developed based on the power plant performance constraints.

The present study was conducted in order to simulate the exact flow conditions found within the prototype. An inherent problem with scaling a flow situation such as this is that the flow dynamics of a scale model cannot be exactly reproduced in the prototype. To circumvent this difficulty, the present experimental setup is designed in such a manner that it is essentially a segment of the prototype. A melting ice plate is used to simulate the vertical ice face of the column while the back wall of the test tank acts as the containment wall of the prototype. Since a segment within the annular space of a prototype would be bounded on both sides by water flowing downward at the same rate, the design of the experimental setup includes continuous belts at the opposing sides of the test tank moving at the same velocity as the water.

General review of the subject

Most of the previous work involving melting of ice was on free convective heat transfer. This work is complicated by water's intriguing feature of reaching a

maximum density at about 4°C. Since existence of maximum density implies that the thermal expansion coefficient β changes its sign, the use of an average value of β then becomes physically unrealistic. More important is the possibility of dual (or "split") flow due to the change in direction of the buoyancy force. Another factor is the change of phase at the solid/liquid interface, which introduces an interfacial velocity and may distort the flow field, thereby affecting the heat transfer rate. Tkachev⁹ was the first to observe the minimum Nusselt number at 5.5°C in his experimental work with melting cylinders. He attributed this minimum to the possibility of two opposing flow regimes within the boundary layer. Schechter and Isbin⁶ experimentally demonstrated the existence of dual flow. From their measurements of the velocity profiles near a warm plate immersed in water, they showed that, at certain temperatures, the inner portion of the boundary layer moved upwards while the outer portion moved downwards. Merk⁵ solved the problem by using an integral method with a moving coordinate system and by considering water as a high Prandtl number fluid. For the case of ice spheres, Merk's analysis indicated that there was a minimum Nusselt number and a complete inversion of flow at a bulk temperature of 4.8°C.

EXPERIMENTAL APPARATUS

General considerations

By the nature of this experiment, there is a need for the maintenance of a constant water temperature and a minimum heat loss in pumping water at a desired rate through the flowmeter to the inlet of the test assembly. PVC pipe was selected for use in all piping because of its low thermal conductivity. Clear Plexiglas was used for the construction of the test tank because of its optical clarity and easy fabrication.

The other factor to be considered was the maintenance of water quality at constant composition throughout the experiments. The high corrosion resistance of aluminum, stainless steel, and brass made their use practical in various load bearing frames and components that were in contact with the water. A small piece of magnesium was placed within the reservoir as a sacrificial metal to protect the aluminum from cathodic reaction with the brass and stainless steel. Distilled water was used to eliminate the problem of chlorine corrosion found in tap water and the production of metal salts that could influence the melting rate of ice. Designs using Teflon and nylon bushing and bearing surfaces, as well as close sliding fits between

associated equipment for easy and accurate assembly of the apparatus, were specified to eliminate the need for organic lubricants which could contaminate the water and affect its physical properties. Apparatus components containing oil, such as gear reducers and flexible shafts, were separated from the rest of the system. This precluded the possibility of introducing detergent oils that would combine with any trace metal salts in the water to create detergent soaps, which would have altered the viscosity and surface tension of the water and introduced unknown factors into the melting characteristics of the test ice sample.

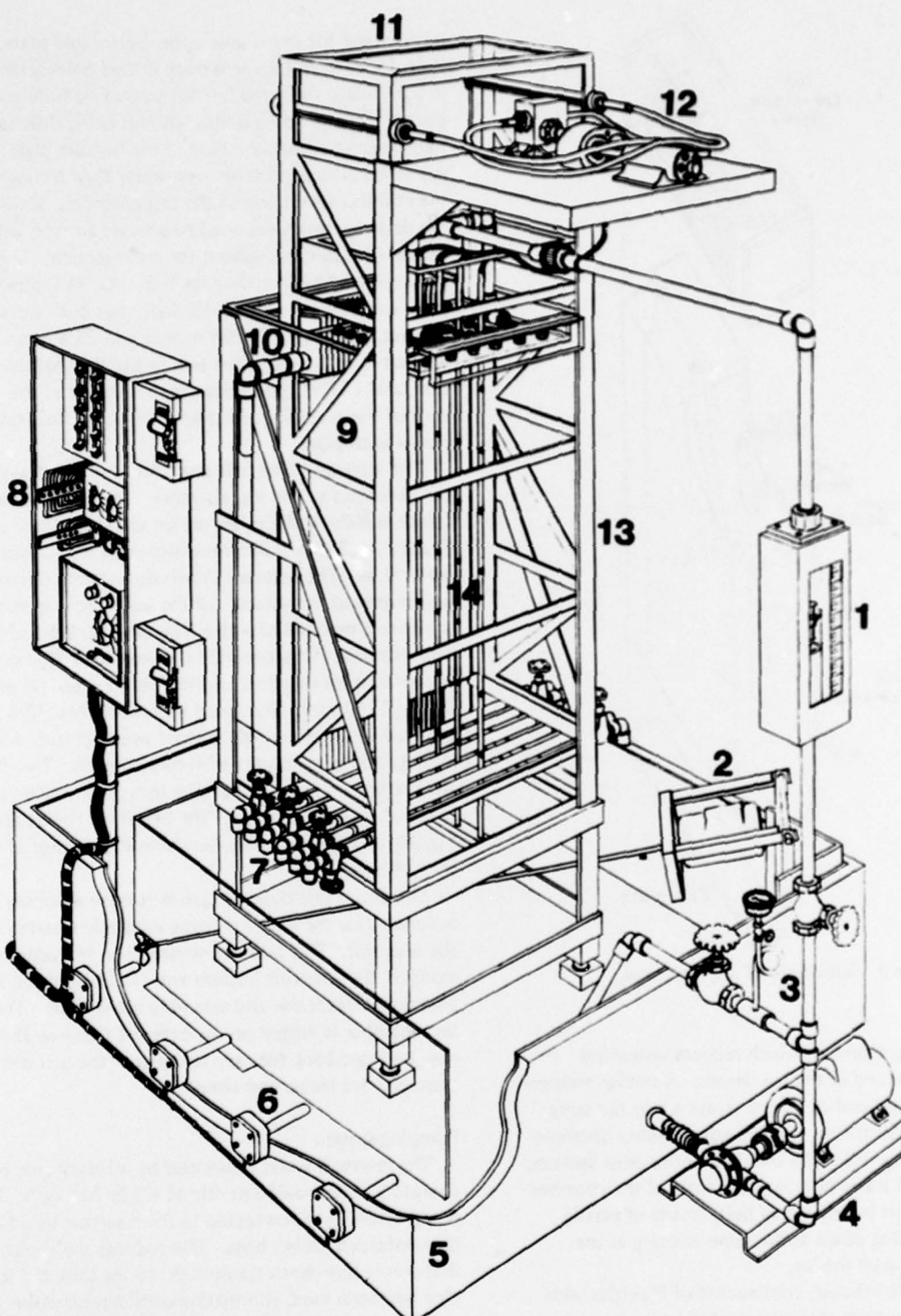
Figure 1 shows the schematic of the experimental setup. It essentially consists of four major parts, i.e. the water reservoir, test chamber assembly, and pumping and control systems. The entire assembly was designed to accommodate a test sample of ice with an exposed vertical face 0.914 m in height and 0.305 m in width.

Water reservoir

The 1.22 x 1.22 x 0.46 m high tank is constructed of welded 4.76-mm aluminum plate. It is supported above the floor by a channel aluminum footing to reduce the heat transfer between the bottom of the tank and the coldroom floor. Both the bottom and side of the tank are insulated externally by 1½-in. thick Styrofoam sheeting. The tank has an operating capacity of 0.473 m³ and is equipped with a 1/3 horsepower mixer. This mixer, through the aid of the baffle system within the reservoir, draws water past the seven 750-W heaters on the two adjoining sides of the tank, pulling it through a passage in the baffle plates into the major open section of the reservoir where it is thoroughly mixed. A thermistor probe, placed within this area, is connected to an on-off controller for the heaters. This probe registers temperature change to within ± 0.05°C.

Test chamber assembly

The test chamber is constructed of 19-mm clear Plexiglas with its external dimensions of 0.495 x 0.445 x 1.238 m high. It contains the ice frame, ice-frame baffles, internal frame belt assembly, drain system and inlet flow distribution box. Figure 2 shows the ice-frame and the baffle device which has the general dimensions of 0.425 m wide x 0.914 m long x 0.152 m thick. The ice frame is also constructed of 19-mm Plexiglas with 8.5-mm aluminum plate mounted in back. The ice sample has a surface area of 0.914 x 0.305 m exposed to melting. The weight of the ice frame is about 19.96 kg and the ice sample weighs about 42.64 kg. The ice-frame slips down within recessed surfaces on the inside of the test chamber and rests upon a baffle arrangement at the



- 1. Rotameter
- 2. Mixer motor
- 3. Flow control valves
- 4. Pump assembly
- 5. Reservoir

- 6. Heaters
- 7. Test chamber drain valves
- 8. Control box
- 9. Ice face
- 10. Overflow pipe

- 11. Internal frame belt assembly
- 12. Belt drive assembly
- 13. Test chamber
- 14. Thermocouple tubes

Figure 1. Schematic of the experimental setup.

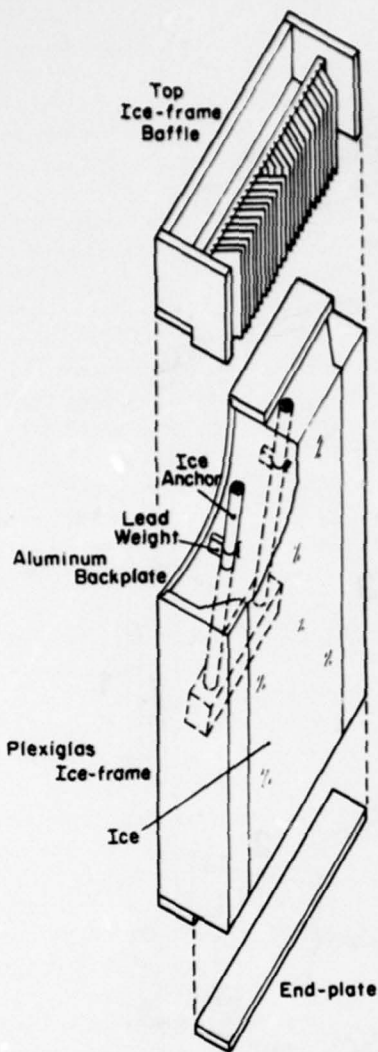


Figure 2. Schematic of the ice frame.

bottom of the chamber, which reduces unwanted erosion on the end of the ice sample. A similar arrangement on the top end of the ice frame serves the same purpose. Uniform flow is achieved by evenly distributing and draining the water over the entire cross section, and simulated water flow on both sides of the chamber is accomplished by the use of belts (made of plastic sheeting) moving down at the same velocity as the water flowing past the ice.

The flow distributor, constructed of Plexiglas with a perforated bottom, sits on top of the test chamber; it has 0.152-m-high sides to control splashing and is fed by a four-outlet header pipe. The water is introduced at right angles to the bottom for even water distribution over the top perforated plate. Spacers are used to vary the distance between the perforated

bottom and the removable upper perforated plate. Both plates have 12.7-mm-diam drilled holes arranged in a mutually staggered fashion so that no flow goes directly through both plates without being diverted at right angles to reach the hole of the bottom plate. The net effect is to provide an even water flow throughout the entire cross section of the test chamber. Similarly the drain system is designed to provide an even withdrawal of water throughout the cross section. This was accomplished by installing six ¾-in. I.D. PVC pipes, evenly spaced, running horizontally out both sides of the test tank. A slit, 0.305 m long and 25.4 mm wide, was cut in each pipe in the side facing the chamber bottom, and 12 PVC gate valves were installed at the ends of the pipes for adjustment for equal flow rates out of each pipe.

The internal frame belt assembly is situated within the perimeter of the test chamber. The belts, made of 0.089-mm-thick Mylar, are set up such that there exists exactly a 0.305 x 0.305-m-square cross section for the water flow. The belts are driven downwards (inside the belt frame) at the velocity of the water flow to simulate an infinite medium of water flow on both sides of the test chamber. This assembly is driven by a $\frac{1}{12}$ -horsepower variable speed d.c. motor with a speed range of 100 to 1750 rpm. The speed is reduced by a 10:1 ratio gear reducer with a single takeoff which in turn drives a 20:1 ratio gear reducer with two takeoffs. Two flexible shafts connect the final gear reducer to the belt roller of 38-mm diameter. The belt drive rollers are capable of operating anywhere within the range of 0.5 to 8.75 rpm.

The entire test chamber and belt drive assembly is supported by the external frame centrally situated in the reservoir. This frame is mounted on threaded brass studs on the reservoir bottom and can be adjusted such that the entire frame and assembly are vertical. The test chamber is hinged on the external frame so that it may be tilted back for easy removal of the belt drive assembly, ice frame and samples.

Pumping system

The reservoir water is pumped by a rotary gear pump operating at its maximum rate of 4.52×10^3 kg/h. The pump assembly is connected to the reservoir by a flexible reinforced rubber hose. This reduces the vibration that would have been transmitted to the tank if a solid pipe had been used, eliminating considerable noise and associated fatigue of welds. The desired amount of water discharged to the test chamber is regulated by a bypass and a main line flow control system. It consists of 1-in.-I.D. brass gate valve leading to the Rotameter and a bypass line upstream of the valve returning the excess

water to the reservoir. The Rotameter is rated from 1.388×10^{-4} to $1.388 \times 10^{-3} \text{ m}^3/\text{s}$.

Electrical control system

All electrical controls for the experiment are arranged together within a control box as an integral part of the experimental setup. Both 120- and 208-V power is supplied through individual disconnect switches. A variable speed control unit is used to regulate the $\frac{1}{12}$ -horsepower d.c. motor for the belt drive. A thermistor on-off control connected to the probe in the reservoir tank operates three relays for the seven heaters in the reservoir. The switch panel provides independent manual control for each of the seven heaters, as well as the mixer motor, rotary gear pump, and temperature control unit.

EXPERIMENTAL PROCEDURE

The ice samples are made by first preparing the ice frame for freezing the distilled water. During this process, the end plates of 12.7-mm-thick Plexiglas are attached to both ends of the ice frame. The plates are held in place by screws with all mating surfaces between the ice frame and end plates being temporarily sealed with silicone elastomer. The ice anchor, made of two PVC tubings leading to threaded holes in a block of Plexiglas, then is put into a position within the ice frame with the ends of the two tubings plugged with rubber stoppers and also sealed with silicone elastomer to prevent water from entering (see Fig. 2). The anchor is kept from moving out of place by lead weights, and the plugged ends of the tubings rest against the end plate. The ice frame is then placed and leveled on the aluminum cold plates; this enables the ice surface to be level with the frame's front surface. Ethylene glycol at -20°C circulates through the 0.28-m-diam coldplates from a constant temperature bath cooled by trichloroethylene at -73.0°C . In filling the ice frame with distilled water, the expansion factor in forming ice from water is also taken into account. During the entire freezing period, the ice frame is covered with an inverted, tightly fitting 38-mm-thick Styrofoam box (without top) and the coldroom temperature is kept at 1.67°C . This allows the ice to form in an upward direction only and eliminates the ice expansion problems associated with the phase transition. Once the ice sample is made (which usually takes four days) the surface is smoothed and evened with a warm copper billet. The excess ice is removed, making the ice surface flush with the ice frame. The ice frame is then placed in a coldroom maintained at -1.0°C and remains there for at least 36 hours with a fan blowing on the backplate to

ensure that the frame and the ice are conditioned to a uniform temperature of -1.0°C .

Prior to the experiment, the end plates and plugs for the ice anchor are removed and the silicone elastomer cleared from the ice frame. Then two stainless steel rods are passed down through the tubes of the ice anchor and threaded into the Plexiglas block to create a handle for placing the ice frame in and removing it from the test reservoir.

In the meantime, the apparatus is being prepared for the experiment. Before the test, the 12 drain valves are calibrated for a specific flow velocity by volumetric flow timing with each one adjusted to equal flow rates at the test temperature. Then the coldroom temperature is raised to 20°C to dry out the water remaining in the valve seats and other parts of the piping system to prevent possible freezeup when the room temperature is brought down to -1.0°C during the experiment. To assure a plug flow in the test chamber, the variable speed drive is adjusted so that the timed movement of the belts matches the calculated water velocity in the chamber. The temperature for the test is set by bringing the reservoir to the desired temperature and maintaining it at that level with the on-off thermistor control.

Prior to the experiment, the coldroom temperature is adjusted to that of the conditioned ice sample (-1.0°C). With the reservoir mixer running, the heater control system is turned on to establish the desired steady state temperature in the reservoir. Once the room is at -1.0°C , the ice frame is brought to the room and weighed, the test tank tilted back, and the ice frame placed into the chamber. The handle attached to the anchor is removed and replaced with two rubber stoppers, and the internal frame belt assembly is slipped into the chamber. The inlet flow distribution box is attached to the side wall of the test chamber and two thermistors are then inserted through the perforated plate and left hanging more or less one-third and two-thirds down the ice frame to measure the variation of temperature in the water during the experiment (the original design with thermocouples was not used). A 1.6-mm Plexiglas sheet is inserted between the belt assembly and ice frame (to prevent melting during rapid filling of the chamber) and the top ice frame baffle is installed. The test chamber is then erected into vertical position and the inlet header pipe and flexible drive shafts are connected.

An experiment is initiated by starting the pump and closing the bypass valve. The belt drive is turned on while the test chamber is being filled. As soon as the water reaches the overflow level, the Plexiglas sheet is removed and the experiment started. The flow rate is adjusted by use of the mainline and bypass valves until there is a small trickle coming out the overflow pipe. The desired flow rate in the test chamber is regulated by

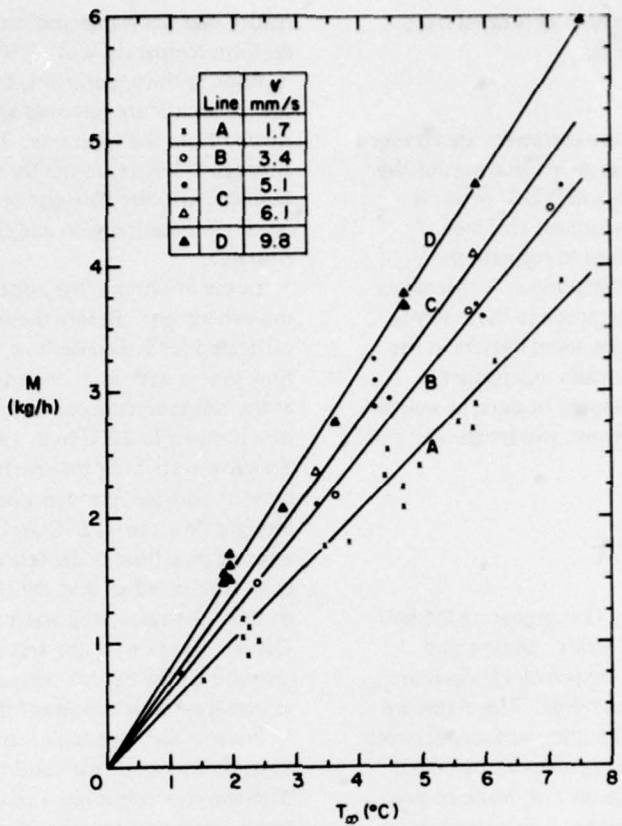


Figure 3. Melting rate as a function of bulk water temperature.

setting the Rotameter reading. The thermistor readings are recorded periodically to see if any variations in temperature existed during the test. The duration of the experiment is determined primarily by the water temperature. For temperatures as low as 1.1°C , experiments last as long as six hours and still do not have an excessive amount of melting. For higher water temperatures, the duration is usually about two or three hours. The experiment is terminated by turning off the gear pump and unplugging the two auxiliary drains located at the bottom of the test chamber. Then the inlet water pipe is disconnected, and the thermistor leads removed from the chamber. The test chamber is tilted back as soon as the water level reaches the bottom of the chamber and the inlet flow distributor, top ice frame baffle and belt drive assembly are removed. Since the ice and the room are maintained at -1.0°C , a thin layer of ice forms between the backplate of the ice frame and the test chamber during the test. To ease removal of the ice frame from the chamber, usually a small amount of hot water is poured directly on this interface. As soon as the ice frame is removed from the test chamber and weighed to determine the amount of

ice melted, the variation of the extent of ice melting is measured at various points on the surface.

EXPERIMENTAL RESULTS

In total, 46 experiments were conducted covering test chamber water velocities v of 1.7 to 9.8 mm/s and bulk water temperatures T_w of 1.11° to 7.50°C . The ice sample prior to the experiment had a smooth surface flush with the ice-frame, but after the experiment, the ice surface was found to be relatively flat with some extra melting along the side near the top. This is attributed to the turbulence created by the inside edges of the ice-frame as ice melts away. In most cases, with the exception of the highest water velocity used in the experiment, the ice surface at the termination of the experiment remains flat indicating even melting. For the case of 9.8-mm/s velocity and the highest temperature (i.e. 7.50°C) there is a greater melting near the water entrance to the test chamber. Experiments 12-13 and 14-15 were run to determine the reproducibility of data under identical conditions. It can be noted that

Table I. Experimental parameters and computed results.

Experiment number	Bulk water temperature T_{∞} (°C)	Experiment duration θ (h)	Water velocity v (mm/s)	Melting rate m (kg/h)	Nusselt number Nu_L	Prandtl number Pr	Reynolds number $Re_L \times 10^3$
1	2.2	6.00	5.1	1.60	396	13.0	3.03
2	1.94	3.00	5.1	1.21	342	13.1	2.80
3	2.22	6.00	1.7	1.07	264	13.0	0.87
4	2.22	6.00	1.7	1.20	296	13.0	0.94
5	4.72	4.00	1.7	2.09	241	12.4	1.02
6*	4.72	4.00	1.7	2.25	259	12.4	1.02
7	1.94	5.00	9.8	1.49	419	13.1	6.00
8	1.94	5.00	9.8	1.60	452	13.1	6.03
9*	1.94	5.00	9.8	1.69	478	13.1	5.65
10	1.83	5.00	9.8	1.47	441	13.1	5.53
11*	1.83	5.00	9.8	1.53	462	13.2	5.46
12	7.50	1.25	9.8	6.11	443	11.8	7.07
13	7.50	1.25	9.8	6.10	442	11.8	7.07
14	4.72	2.50	9.8	3.76	437	12.4	6.50
15	4.72	2.50	9.8	3.67	424	12.4	6.50
16	2.77	4.00	9.8	2.07	408	12.6	6.10
17	3.61	3.00	9.8	2.75	416	12.7	6.64
18	5.83	2.00	9.8	4.65	433	12.2	7.32
19	5.83	2.50	5.1	3.68	344	12.2	3.40
20	7.20	2.00	5.1	4.64	350	11.9	3.54
21	4.44	3.00	5.1	2.95	362	11.9	3.25
22	3.33	4.50	5.1	2.10	343	12.3	3.15
23	1.11	7.00	5.1	0.76	377	13.3	2.91
24	5.83	2.50	1.7	2.92	290	12.2	1.13
25	7.22	2.00	1.7	3.88	308	11.9	1.18
26	4.44	3.00	1.7	2.52	329	12.5	1.12
27	5.56	1.75	1.7	2.76	268	12.3	1.12
28	5.80	2.75	1.7	2.71	252	12.2	1.17
29	3.47	5.00	1.7	1.79	280	12.7	1.10
30	2.42	5.00	1.7	1.02	227	13.0	1.05
31	2.25	5.00	1.7	0.92	222	13.0	1.05
32	3.84	3.00	1.7	1.83	258	12.6	1.10
33	4.41	3.00	1.7	2.33	285	12.5	1.13
34	4.95	3.00	1.7	2.43	265	12.4	1.15
35	6.18	2.50	1.7	3.27	284	12.1	1.19
36	2.25	4.75	1.7	1.14	277	13.0	1.05
37	1.54	5.00	1.7	0.73	261	13.2	1.28
38	3.30	2.50	6.1	2.35	370	12.8	4.68
39	5.80	2.17	6.1	4.08	379	12.2	3.74
40	5.75	3.00	3.4	3.66	343	12.2	2.08
41	7.04	2.58	3.4	4.49	341	11.9	2.12
42	3.64	4.42	3.4	2.17	324	12.7	1.92
43	2.40	5.00	3.4	1.47	334	13.0	1.84
44	4.43	2.50	5.1	2.89	352	12.5	2.95
45	4.43	2.50	5.1	3.09	376	12.5	2.95
46	4.43	2.50	5.1	3.25	369	12.5	2.95

* Experiments without belts operating.

the apparatus was able to provide consistent data. A few experimental runs were also conducted without the belts moving to assess the effect of the buildup of side boundaries on the melting rate. To simulate the prototype operation conditions more closely, all other experiments were conducted with the belts moving. Table I shows the experimental conditions and the

calculated results. Figure 3 shows the variation of melting rate M with T_{∞} , using v as a parameter. All the curves are extrapolated to point zero for no melting at 0°C. The data show a great deal of scattering, demonstrating the possibility that varying extents of turbulence were introduced at the entrance of the test chamber. As mentioned earlier, the water must be

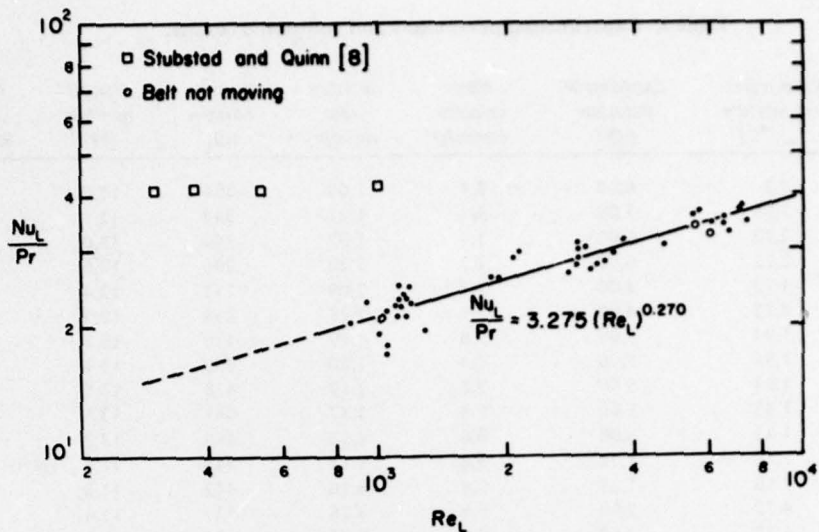


Figure 4. Relation between $\frac{Nu_L}{Pr}$ and Re_L .

maintained at an overflow level during the entire test period. Otherwise, there will be a gap between the inlet water distributor and the water level in the test chamber, and the water will be running down to the chamber, thus creating turbulence and promoting a higher rate of heat transfer. Also the low sensitivity of the weighing scales has contributed to the inconsistency of the data. Regardless of the scattering of the data, however, the trends clearly show that the ice melting rate has a strong dependence on bulk water temperature and water velocity.

The experimental results are expressed in terms of an average heat transfer coefficient h defined as

$$h = \frac{q_s + q_f}{A \Delta T \theta} \quad (1)$$

where q_s = sensible heat required to raise the ice from initial temperature T_i ($< 0^\circ\text{C}$) to the melting temperature T_m ($= 0^\circ\text{C}$)

q_f = heat of fusion associated with melting

A = area of the melting surface

ΔT = temperature difference between T_∞ and T_m (since $T_m = 0^\circ\text{C}$, $\Delta T = T_\infty$)

θ = the time duration of the experiment.

A Reynolds number ($Re_L = v \rho_L / \mu$) based on ice plate height is used to define the flow characteristics, where ρ and μ are the water density and viscosity, respectively. The physical properties are evaluated at the arithmetic mean of bulk water temperature T_∞ and melting temperature T_m or $T_m/2$. For each experiment, the weight of ice melted W , as well as T_∞ , θ and the flow rate are

recorded. The amount of ice melted W is used to compute $q_s = W c_i (T_m - T_i)$, and $q_f = WL_f$ where c_i , T_i and L_f are the specific heat, initial temperature, and latent heat of fusion of the ice, respectively. Figure 4 shows a correlation between Nu_L/Pr and Re_L in which Nu_L and Re_L are evaluated based on height of the plate. The relation can be fairly represented by

$$\frac{Nu_L}{Pr} = 3.275 (Re_L)^{0.270} \quad (2)$$

with a correlation coefficient of 0.843. The relatively low value of the correlation coefficient is essentially due to the difficulty in ascertaining the accuracy in the temperature measurement, especially when the bulk water temperature is near the melting temperature. For $\Delta T = 1^\circ\text{C}$, a 0.1°C error introduces a 10% variation in the heat transfer coefficient, assuming that the ice weighing is reproducible. A few experimental data without the belts moving are also indicated in Figure 4. It can be seen that, although there seems to be some effect of the moving belts on the ice melting rate, the effect of the two side plates (belts) does not reduce the heat transfer rate noticeably, and in fact the data are all within the experimental range from one to another. A partial explanation is that there would be minimal frictional resistance to flow with a very thin boundary layer buildup because the belts are made of smooth Mylar sheets. Another explanation is that the ice plate is wide enough to consider the boundary effect insignificant.

DISCUSSION AND COMPARISON OF RESULTS

As indicated in the *Introduction*, there have been no experimental forced flow studies of a vertical melting plate. However, Yen and Tien¹¹ solved, in an analytical study, the laminar heat transfer problem over a horizontal melting plate with a linear boundary layer velocity distribution, i.e. $v_x = By$ where v_x is the velocity along the plate. The equation of energy was solved analytically and the Nusselt number can be expressed by

$$Nu_L = \frac{L}{a_n} \left(\frac{B}{9\alpha} \right)^{1/3}. \quad (3)$$

where L is plate length. The value of a_n is evaluated from the integral

$$a_n = \int_0^{\infty} \exp(-\lambda^3 + \beta\lambda/a_n) d\lambda \quad (4)$$

where $\beta = c(T_{\infty} - T_m)/L_f$ and can be regarded as a melting parameter. The value of a_n is found to be a function of β . By approximating the value of B with τ_w/μ , where τ_w is ice-water interface shear stress and μ is the dynamic viscosity of water, the ratio of Nu_L (with melting) to Nu_0 (without melting) is found to be

$$\frac{Nu_L}{Nu_0} = \frac{a_0}{a_n} \left(\frac{\tau_w}{\tau_0} \right)^{1/3} \quad (5)$$

where

$$a_0 = \int_0^{\infty} \exp(-\lambda^3) d\lambda. \quad (6)$$

Since the velocity profile is assumed to be comparable to the temperature profile and τ_0 is proportional to the velocity gradient, eq 5 can be reduced to

$$\frac{Nu_L}{Nu_0} = \left(\frac{a_0}{a_n} \right)^{4/3}. \quad (7)$$

For the case of flow over a flat plate with no pressure gradient and no mass transfer across the plate, the Nusselt number is given by Schlichting⁷ as

$$Nu_0 = 0.664 (\Pr)^{1/3} (Re_L)^{1/2}. \quad (8)$$

Therefore, the Nusselt number in case of melting is

$$Nu_L = 0.664 \left(\frac{a_0}{a_n} \right)^{4/3} (\Pr)^{1/3} (Re_L)^{1/2}. \quad (9)$$

Figure 5 shows a comparison of eq 8 and 9 and the experimental data of the present investigation. Experimental conditions are used to evaluate the value of the parameter $(a_0/a_n)^{4/3}$ in eq 9, which depends on $c T_{\infty}/L_f$. Since $c T_{\infty}/L_f$ varies in the experiments between 0.014 and 0.094, the effect of $(a_0/a_n)^{4/3}$ on the values of Nu_L is rather small. However, for $c T_{\infty}/L_f = 1.0$ the reduction in heat transfer can be quite large, approximately amounting to 42%. As can be noted from the figure, the present experimental results are about four to five times greater than those predicted from a horizontal flat melting plate. The results can be fairly represented by

$$\frac{Nu_L}{(\Pr)^{1/3}} = 16.5 (Re_L)^{0.279} \quad (10)$$

with a moderate correlation coefficient of 0.895.

A few data points from Stubstad and Quinn⁸ are shown in Figure 4. The disagreement with the present data is apparent. In their experiment, a cylindrical column of ice 3 m in height and of 1.83 m initial diameter was used. For a given mass flow rate, the annular space between the tank wall and ice surface increases as melting progresses; therefore, for a given experiment the value of Re_L is reduced. In their computation of an average heat transfer coefficient, the assumption was made that there was no change in height during the experiment. (In reality, this is not true.) The value of h is computed from

$$h = \left(\frac{\rho_i L_f}{T_{\infty}} \right) \left(\frac{\Delta R}{\Delta \theta} \right) \quad (11)$$

where T_{∞} is average bulk water temperature. The value of incremental change of ice radius R with time, obtained by considering the volume and mass change of ice, can be finally expressed as

$$\Delta R = R(\theta_1) - \sqrt{R^2(\theta_1) - (\Delta \theta / \rho_i \pi L)(dM_i/d\theta)} \quad (12)$$

where M_i is the initial ice mass in the tank. From this relationship it is possible to determine the average change of the radius of the ice cylinder during any time interval from θ_1 to θ_2 . The discrepancy between these data and the present data can be attributed largely to

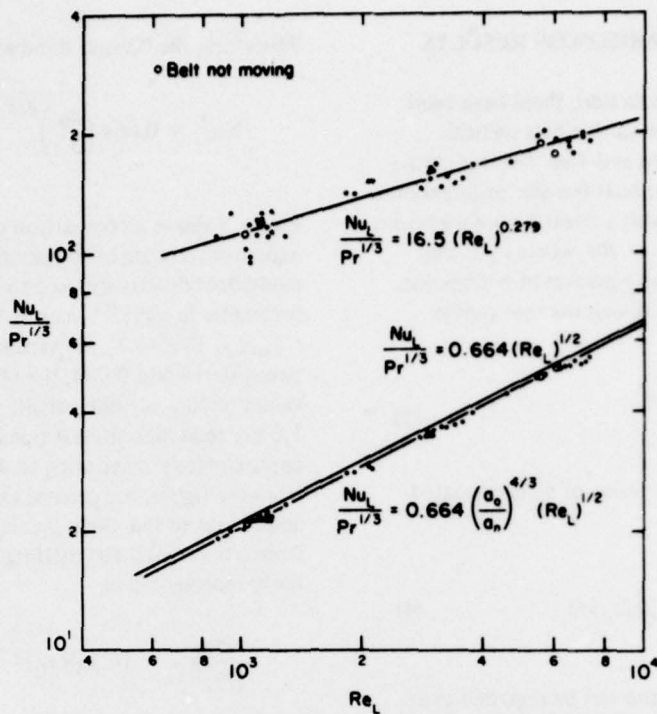


Figure 5. Comparison of present data with computed values from horizontal plate.

the assumption of constant height and the method of obtaining the variation of R with the water level change associated with the phase change. The higher values of Nu_L are also due to the high degree of turbulence of the entering water spraying directly down from the nozzle into the annular gap.

As mentioned in the *Introduction*, quite a few investigators have worked on the free convective melting heat transfer problem. Vanier and Tien¹⁰ studied the problem both analytically and experimentally. By studying a combination of plate and bulk water temperatures, they were able to identify the various flow regions created by the unique property of water which exhibits a maximum density at about 4°C. With boundary layer approximations, including the effect of density inversion, and the use of similarity transformation, they solved the equations of motion and energy numerically. The Nusselt number was found and expressed as

$$Nu_L = \frac{2\sqrt{2}}{3} (Gr)^{1/4} [-H'(0)] \quad (13)$$

where the Grashof number is always positive and is defined as

$$Gr = \frac{gL^3 |\beta_m (T_p - T_\infty)|}{\nu^2}$$

where T_p is plate temperature, and ν the kinematic viscosity. β_m is defined by

$$\beta_m = \frac{\beta_1 + 2\beta_2 T_m + 3\beta_3 T_m^2}{1 + \beta_1 T_m + \beta_2 T_m^2 + \beta_3 T_m^3} \quad (15)$$

in which β_1 , β_2 and β_3 are the coefficients in the cubic expression of the density-temperature relationship of water and $H'(0)$ is the dimensionless temperature gradient at the plate. For the case of $T_p = 0^\circ\text{C}$ (equivalent to the case of melting $T_m = 0^\circ\text{C}$), Vanier and Tien's numerical results (after scaling to the present experimental plate height) are shown in Figure 6.

The most recent experimental study of natural convection flow over a vertical ice slab immersed in cold water has been reported by Bendell and Gebhart.¹ In this study, the effect of the bulk water temperature, especially in the vicinity of the density extremum, on heat transfer was determined. Also, the effect of the density maximum on flow direction and bulk water

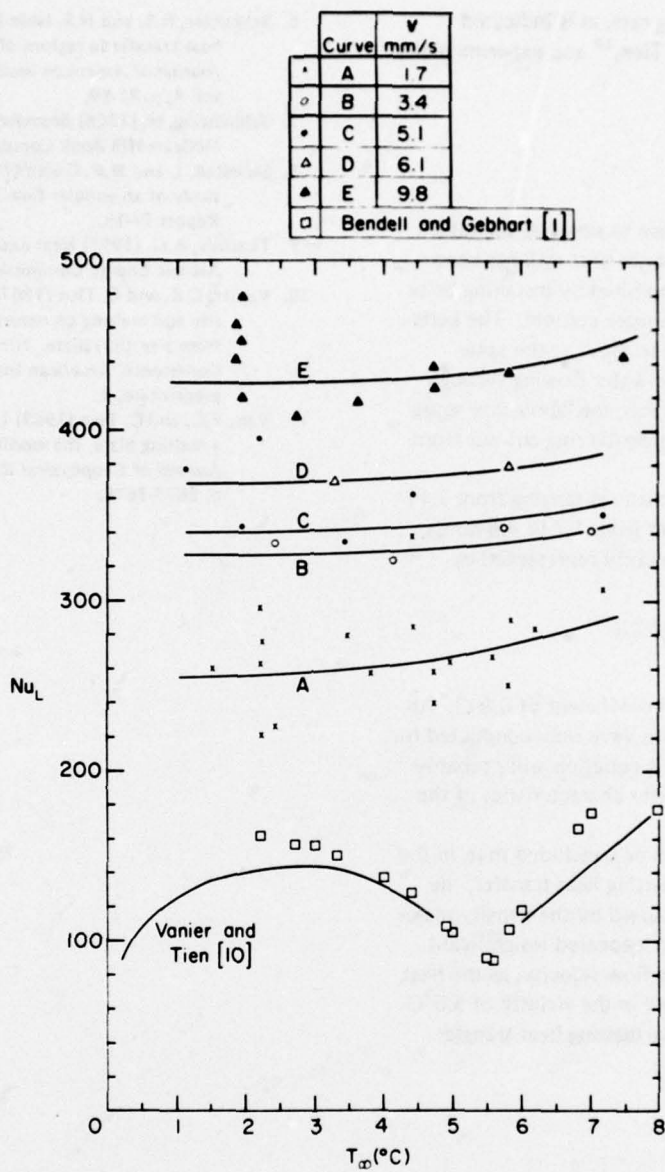


Figure 6. Comparison of present data with those from free convection studies.

temperature where upflow changes to downflow was determined. They compared their experimental results with the analytical work of Gebhart and Mollendorf³ and found a mean magnitude of deviation of 5.6%. Their experimental results are also shown in Figure 6 along with the present results. It can be seen that the work of Bendell and Gebhart agrees with the analytical work of Vanier and Tien¹⁰ fairly well. It also can be noted that, for the case of forced motion, there is a significant increase in heat transfer rate over free convection even with a minimal velocity of 1.7 mm/s.

The greater scattering of data, especially at the lower extreme of the temperature used in this experiment, can be partially attributed to the inaccuracy in the temperature measurement. A small error in the absolute temperature measurement can cause a great percentage of deviation and thus create a much greater magnitude of scattering. However, the effect of flow on the melting heat transfer can easily be visualized in Figures 3, 4 and 5. For the temperature range covered in this study it seems that the change in the direction of flow due to buoyancy forces has exhibited no

significant effect on melting rate, as is indicated numerically by Vanier and Tien,¹⁰ and experimentally by Bendell and Gebhart.¹

CONCLUSIONS

1. An experimental device to simulate the rather large dimensions of a prototype heat sink has been developed. This was accomplished by installing belts on two opposite sides of a square column. The belts were designed and adjusted to move at the same direction and velocity as the water flowing through the test chamber. In doing this, the laboratory setup could be considered as a segmental ring cut out from the proposed prototype.
2. For bulk water temperatures ranging from 1.1 to 7.5°C and water velocities from 1.7 to 9.8 mm/s, the present results could be fairly represented by

$$\frac{Nu_L}{Pr} = 3.275 (Re_L)^{0.270}$$

with a moderate correlation coefficient of 0.843. Although the experimental runs were only conducted for one specific plate height, this equation will probably predict the actual heat transfer characteristics of the prototype.

3. From this study it can be concluded that, in the case of forced convective melting heat transfer, the effect of buoyancy forces caused by the density maximum at 4°C on heat transfer appeared insignificant. This is true even at very low flow velocity, as the heat transfer is drastically reduced in the vicinity of 5.6°C in the case of free convective melting heat transfer.

LITERATURE CITED

1. Bendell, M.S. and B. Gebhart (1976) Heat transfer and its melting in ambient water near its density extremum. *International Journal of Heat and Mass Transfer*, vol. 19, p. 1081-1087.
2. Brown, J.L. and W.F. Quinn (1975) An annular flow ice-water model heat sink. CRREL Special Report 236, AD A015468.
3. Gebhart, B. and J. Mollendorf (in preparation) Buoyancy induced flow in a liquid under conditions in which a density extrema may occur. Submitted to *Journal of Fluid Mechanics*.
4. Grande, E. (1975) Analysis and conceptual design of practical ice water heat sinks. CRREL Special Report 221, AD A009498.
5. Merk, H.J. (1954) The influence of melting and anomalous expansion on thermal convection in laminar boundary layers. *Applied Scientific Research*, section A, vol. 4, p. 435-452.
6. Schechter, R.S. and H.S. Isbin (1958) Natural convection heat transfer in regions of maximum fluid density. *Journal of American Institute of Chemical Engineers*, vol. 4, p. 81-89.
7. Schlichting, H. (1968) *Boundary layer theory*. New York: McGraw-Hill Book Company.
8. Stubstad, J. and W.F. Quinn (1977) An experimental scaling study of an annular flow ice-water heat sink. CRREL Report 77-15.
9. Tkachev, A.G. (1953) Heat exchange in melting of ice. Atomic Energy Commission Translation 3405.
10. Vanier, C.R. and C. Tien (1967) Effect of maximum density and melting on natural convection heat transfer from a vertical plate. Ninth National Heat Transfer Conference, American Institute of Chemical Engineers, preprint no. 3.
11. Yen, Y.C. and C. Tien (1963) Laminar heat transfer over a melting plate, the modified Leveque problem. *Journal of Geophysical Research*, vol. 68, no. 12, p. 3673-3678.

In accordance with letter from DAEN-RDC, DAEN-ASI dated 22 July 1977, Subject: Facsimile Catalog Cards for Laboratory Technical Publications, a facsimile catalog card in Library of Congress MARC format is reproduced below.

GB
2405 Yen, Yin-Chao
.C6 Heat transfer over a vertical melting plate /
Report by Y-C. Yen and M. M. Hart. Hanover, N.H.: U.S.
77-32 Cold Regions Research and Engineering Laboratory,
 1977.
 v, 12p.: ill. ; 27cm. (CRREL Report ; 77-32)
 Prepared for In-House Laboratory Independent
 Research under DA Project no. 4A161101A91D.
 Literature cited: p. 12.
 1. Heat sinks. 2. Heat transfer. 3. Ice.
 4. Melting. I. Hart, M. M. II. United States.
 Army Cold Regions Research and Engineering
 Laboratory, Hanover, N.H. III. Title IV. Series